Technological innovation in the recovery and analysis of 3D forensic footwear evidence: structure from motion (SfM) photogrammetry

Hannah Larsen[1], Marcin Budka[2], Matthew R. Bennett[1]

[1]Department of Life and Environmental Sciences, Faculty of Science and Technology, Bournemouth University, Talbot Campus, Poole, BH12 5BB, UK.

[2]Department of Data Science, Faculty of Science and Technology, Bournemouth University, Talbot Campus, Poole, BH12 5BB, UK.

Abstract

The recovery of three-dimensional footwear impressions at crime scenes can be a challenge but can also yield important investigative data. Traditional methods involve casting 3D impressions but these methods have limitations: the trace is usually destroyed during capture; the process can be time consuming, with a risk of failure; and the resultant cast is bulky and therefore difficult to share and store. The use of Structure from Motion (SfM) photogrammetry has been used widely to capture fossil footprints in the geological record and while there is a small body of work advocating its use in forensic practice the full potential of this technique has yet to be realised in an operational context. The availability of affordable software is one limiting factor and here we report the availability of a bespoke freeware for SfM recovery and subsequent analysis of for footwear evidence (DigTrace). Our aim here is not to provide a rigorous comparison of SfM methods to other recovery methods, but more to illustrate the potential while also documenting the typical workflows and potential errors associated with an SfM based approach. By doing so we hope to encourage further research, experimentation and ultimately adoption by practitioners.

Keywords

Forensic Science; Footwear Evidence; SfM Photogrammetry; Accuracy; Precision

1 Introduction

The UK National Policing Improvement Agency (NPIA) [1] reported footwear as the second most common type of evidence found at crime scenes. Despite the frequency with which such evidence is found technical innovation around the capture and analysis of footwear has fallen behind other types of evidence as a quick survey of three forensic journals illustrates, namely: Journal of Forensic Identification, Journal of Forensic Science and Forensic Science International. Between 2018 and 2019 only 1.3% of published papers had a footwear focus

compared to 22.4% dealing with for example fingerprints, yet footwear traces are perhaps more common [2] and less easily mitigated against by the criminal.

Footwear evidence fall into either 2D traces or 3D impressions which are sometimes referred to as plastic impressions [2]. Traditional method of collecting 3D footwear evidence involve casting, or alternatively a high quality orthogonal 2D photograph is taken. Casting is an invasive and labour-intensive method which relies on an experience-based protocol developed by individual practitioners [2]. The limits of precision and accuracy are not well researched, or established, compared to the errors associated with other types of trace evidence recovery.

Alternative methods of 3D capture now exist such as structured light, optical laser scans and photogrammetry [3,4], and an argument can now be made that the collection of footwear evidence should embrace this technical innovation with due benefit. This is particularly true in light of recent use of footwear evidence as part of intelligence-led policing initiatives [4]. In the UK, a number of police forces have either introduced, or are actively exploring, digital custody footwear capture linked to rapid pattern-matching algorithms that provide potential investigative leads for timely decision-making and/or suspect interrogation. At present 3D traces are not easily compatible with such systems, which are based on black and white impressions, but adoption of digital capture could change this. There has been previous discussion of using 3D scanners for footwear evidence [e.g., 5,6] and for broader forensic uses [4] such as external injuries on a body. Buck et al [4] provides a comprehensive validation of 3D acquisition techniques including multiple types of scanning equipment for the recovery of forensic materials. The capital cost of scanning equipment is falling rapidly and scanners are now available at many price points. Scanners do still require investment in equipment, software, and training but plug and play scanners are now offering examiners the benefit of seeing direct results, aiding in lessening training requirements. An alternative to scanning methods is 3D capture using Structure from Motion (SfM) photogrammetry [4,8,9,10,11,12] which requires nothing more than a standard digital single lens reflex camera such as that used already by Crime Scene Investigators (CSI), appropriate software and IT infrastructure to run it on. A series of oblique photographs from different angles are taken of a target trace and returned to the laboratory where a 3D model is then computed. The crime scene camera is already a standard component of a forensic practitioner's kit, little training is required for image capture, and free software solutions are now available to build and analyse such models. Admittedly investment in IT infrastructure and training is required to build the 3D model from the photographs, but this can be limited to specialist officers. In addition, not seeing direct results at the scene may not suit every examiner and potentially extend training requirements.

The potential of Structure from Motion photogrammetry was recognised in 2000 by Pollefeys et al. [13] and has been illustrated since in a number of papers [14,15] but momentum has only just begun to build around this potential within forensic science. Villa and Jacobsen [16]

discussed the contribution that photogrammetry could make across a range of forensic evidence types (see also: [3,17]). Clearly, the accuracy, precision and operational reliability of any new technique needs to be full explored and documented to ensure that evidence collected is both robust and able to withstand legal scrutiny. Larsen and Bennett [18] have previously addressed this, and while more research is needed our aim here is to illustrate the required workflow, potential pitfalls and to provide practical guidance for those practitioners wishing to experiment with his technology. More than anything else we wish to illustrate the capability of SfM to capture footwear evidence from a range of environments. In light of this, the current paper is structured around three themes: a review of SfM workflow, a review of potential errors and a series of case studies.

2 SfM Methodology

There are several commercial and non-commercial options for SfM capture. They all work on the same basic principle, that a series of oblique digital photographs are taken of a target trace and that an algorithm then matches either single, or groups of pixels, to compute the camera location before placing those pixel groupings in 3D space. This network of located pixels is then used to create a denser point cloud with each point on the surface of the trace having an *x*, *y*, and *z* coordinate. In addition, colour information is usually stored as RGB values for each of these points or vertices.

The SfM solution used in this paper is DigTrace (www.digtrace.co.uk) which is a freeware option created at Bournemouth University with support from the Natural Environment Research Council and project partners at the UK Home Office and UK National Crime Agency. It uses openMVG [19] (Open Multiple View Geometry) as the SfM engine and has a range of additional tools specifically for the analysis of 3D footwear impressions. To be clear however, there are other freeware and commercial SfM software solutions and the industry standard is currently provided by Agisoft Metashape (https://www.agisoft.com/). These also provide good model building capacity, but the tools available are generic to the 3D industry as a whole rather than specific to the analysis of forensic footwear. There are also a wide range of commercial and freeware packages for viewing 3D models once they have been created (Table 1). The typical workflow using the DigTrace SfM approach is illustrated in Figure 1 but is similar in broad terms to any SfM software.

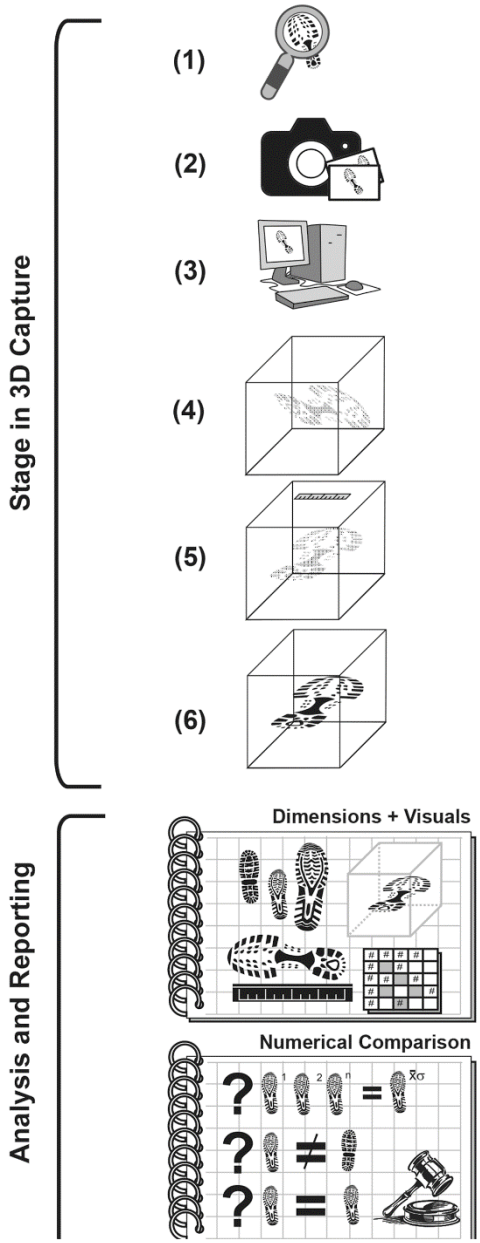

Figure 1: Typical workflow for SfM photogrammetry with particular reference to DigTrace. The steps are: (1) to identify the trace to be recovered; (2), take the necessary photographs; (3) upload those photographs into appropriate SfM software and build a 3D point cloud of the surface of the trace; (4) correct the plane of the model so that is orthogonal when viewed from above; (5) scale the point cloud; (6) surface the point cloud; and (7) perform whatever analysis is required.

Software Name	Description	Specific tools	Key Benefits or Limitations
Model Building			
DigTrace	Freeware - Designed for use with footwear traces in a forensic context	Model Building, visualising, analysis tools, model comparison	Tools specific to footwear analysis
Agisoft Metashape	Commercial software – generic use, high quality options	Model building, visualising, analysis tools	Extensive options and editing tools
Photomodeler	Commercial software – generic use, high quality options	Model building, visualising, analysis tools	Affordable commercial option
Reality Capture	Commercial software – generic use, high quality options	Model Building, visualising, analysis tools	Simple and intuitive user interface
3DR Zephyr	Commercial software – generic use	Model Building, visualising, analysis tools	Built for user-friendliness
VisualSFM	Freeware – generic use	Model Building, visualising, analysis tools	Simple to use
Regard3D	Freeware – generic use	Model Building, visualising, analysis tools	Comprehensive editing tools
MicMac	Freeware – generic use	Model Building, visualising, analysis tools, surface reconstruction	Most suitable for professional or academic users
Multi View Environment	Freeware – generic use	Model Building, visualising, analysis tools,	Complicated User Interface
Meshroom	Freeware – generic use	Model Building, visualising, analysis tools	Easy to use workflow
COLMAP	Freeware – generic use	Model Building, visualising,	High Quality options reduce ease of use
Model Visualising			
Meshlab	Freeware - Processing and Editing 3D triangular meshes (ref)	Used by authors for surfacing models built using DigTrace	
CloudCompare	Freeware - Processing and Editing 3D triangular meshes	Used by authors for Cloud to cloud comparisons for models built using DigTrace, contour-lines and depth maps generation	
Paraview	Freeware - Processing and Editing 3D triangular mesh	Used by authors for contour-lines and depth maps generation	

Table 1: Summary of software options for creating and viewing SfM 3D models, current in the autumn of 2020 [20,21] There has been a proliferation of photogrammetry software for drone mapping which in some instances can be used for close range, these have, however, not been included here.

The first step involves identifying the target(s) trace(s). The second step involves taking 20 to 30 oblique photographs of the target with a digital camera from Smartphone to dSLR quality (Fig. 1). Whilst a dSLR would be recommended, with advances in technology a smartphone camera would suffice. This is particularly pertinent due to material availability at a crime scene. For example, if a crime scene footprint has been found in snow which is melting and a dSLR camera is located in the police station 10 miles away, then the quality of photographs captured from a smartphone is perfectly adequate to avoid loss of evidence. This is a quick process and takes on average 69 ± 0.7 seconds per target (based on: 50 models, 30 photographs per models). In terms of camera the only essential requirement is that the sensor size (width in mm) is known, and this can usually be obtained from the camera specifications or the internet. In general, the better quality the camera in terms of sensor size and pixel density the better the 3D model will be. However, as the individual image file sizes increase, so does the computational power required to build the 3D model and subsequently work with it. A standard CSI quality dSLR gives accurate and precise results without undue computational load, as does a high-quality smart phone camera.

The precise orientation of the photographs does not need to be constrained, although we recommend when using DigTrace that the protocol shown in Figure 2A is used to ensure a good quality model is attained. If a trace/track is deep and has undercut sides they may go unrecorded unless the face is shown in at least two pictures and this may require some low angled pictures to be taken. The photo procedure involves taking sharp, well-lit, overlapping photos (at least 30% overlap) from around and above the impression with care to take photos extending well beyond the impression itself. A scale bar should be included in the photographs but does not need to be in the same plane as the impression but should not be moved during the procedure. Some commercial software options (e.g., Agisoft Metashape) use scales with machine readable targets on them that help with scaling.

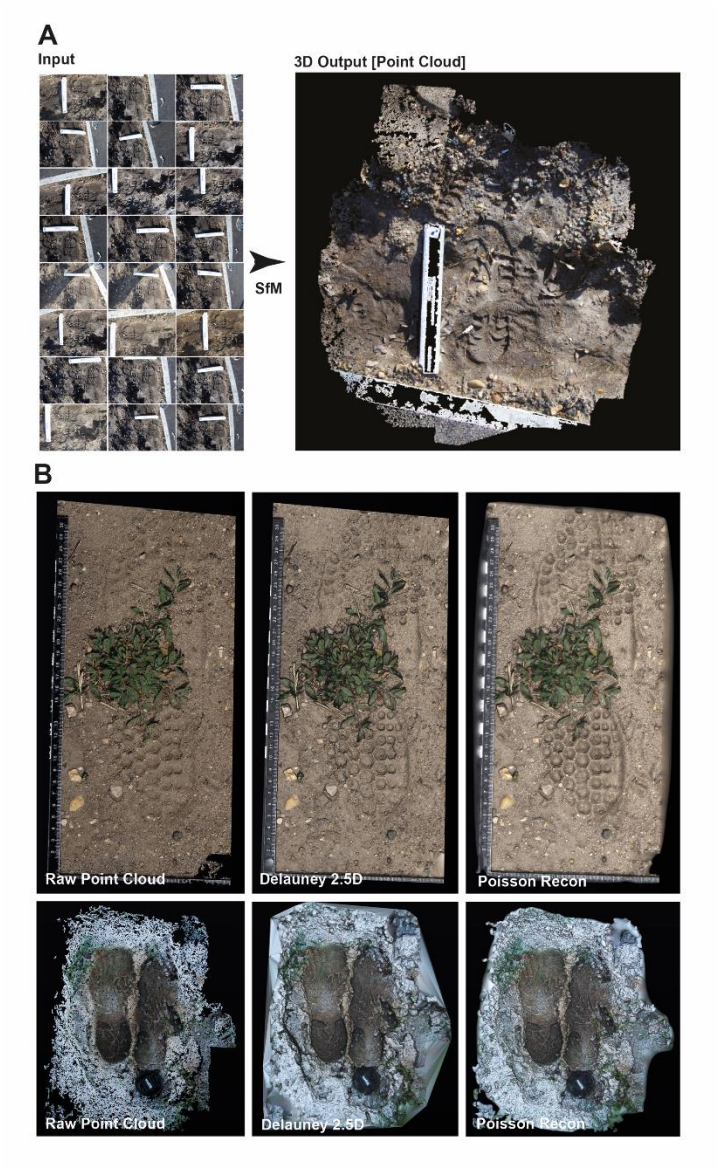

Figure 2: Creating 3D models using SfM. ***A.*** *Generic illustration of how 24 photographs from different angles and positions can create a 3D point cloud.* ***B.*** *Illustration of the differences between point cloud and two commonly used surfacing algorithms. The upper models are made in loose sandy soil and the lower models in melting snow. Note that the two algorithms give similar results.*

On return to the laboratory the photographs pertaining to a given trace(s) are sorted into a single folder and that folder is named appropriately. In DigTrace the folder name is the subsequent model name. This folder is then uploaded into DigTrace, or the commercial alternatives, and a model is made. The time it takes to create a 3D model varies with the number of photographs, their size and the computational power of the computer used and can vary accordingly from as little as a few minutes to over 20 minutes. Most software solutions allow for batch processing, such that all the models from a scene for example can be run over

night [3; Fig. 2A]. The next step (Step-Four) is one of the most important and that is to correct the plane of the 3D model such that it is orthogonal to the viewer (Fig. 1). It is equivalent to ensuring that a forensic photograph is taken perpendicular to the subject. Tools to do this simply and accurately in commercial software such as Agisoft Metashape are limited, in DigTrace however the principal plane through the point cloud is calculated automatically and the transformation needed to move this into the orthogonal plane is then applied to all the points in the cloud (i.e., auto-rectified). If this is not done, then subsequent colour renders by depth will not bring out the track detail. There may be cases where the original slope is important to understand a sequence of tracks, this is not the same as the 3D model orientation and to create an accurate slope one must have *x*, *y* and *z* locational data for reference points within the model to calibrate the slope correctly. Crucially this needs to be anticipated at the scene when the photographs are first taken.

The cloud of points produced in this way is unscaled, and the scale bar included in the images must now be used to create a real-world distance-spacing for the cloud. This should only be done once the plane of the model has been correct to ensure that true distance is being measured. A known distance on the scale bar is measured on the 3D model and a scaling factor calculated and applied to all the points. The point cloud is the raw data, and any measurements or analysis will only be as good as the coverage of points over the original target. Each point in the cloud has an RGB-value assigned to it. When the observer zooms into a point cloud by increasing the magnification the points become more widely spaced and the detail is lost. As a consequence, most clouds are interpolated or surfaced via a mesh for visualisation purposes. There are surfacing or triangulating algorithms that can be applied, common ones widely implemented in the software listed in Table 1 are Poisson Surface Reconstruction [22] and 2.5D Delaunay Triangulation [23,24; Fig. 2B]. There is an extensive literature around the relative merits of different surface meshing technique. As it has been extensively done in the past no further details are discussed here, but two visual examples have been provided [25; Fig 2B].

2.1 Accuracy and Reliability

Ideally any measure of quality assurance for a 3D model of a trace, commonly referred to as a 2.5D surface [3], should be based on departure of the model surfaced in three dimensions (*x*, *y* and *z*) from the original surface. We can break-down this into four elements or potential sources of error:

(1) Spatial placement accuracy and precision errors (Error-1). These errors measure both the accurate and consistent placement of a component point on an SfM model. Does a point plot with the same Euclidean coordinates every time and do these match the coordinates on the original point? Or put another way does an object of known

dimensions on the original surface have the same dimensions on the SfM model? This is a function of such things as: the SfM algorithm used; the quality of the individual images; the coverage and overlap of images; the number of images; and the variation in pixel diversity across the target. Software and equipment come into play here, but also the operator.

(2) Scaling accuracy/precision errors (Error-2). All models made via photogrammetry must be scaled using a scale-bar (or via machine-readable targets a known distance apart) and this can be a source of error. In theory we can test a model's comparative accuracy by comparing linear measurements between points in the SfM cloud with those distance on the original surface. Additionally, to be precise a SfM model built repeatedly from different sets of photographs should give a consistent set of values for point to point distances. It is unusual for models of the same subject to be made more than once so this often goes unrecorded.

(3) Point-cloud coverage (Error-3). Clearly, a model full of holes or blank areas (zero points) has no 3D data to provide in those areas. Small holes are not uncommon in 3D models. If a surface is to uniform, with little textural variety, matching pixel clusters between images will fail, leading to a hole. Reflections from damp or shiny surfaces can also cause a problem, as can variable-shadows or flat light. If a model is surfaced or interpolated as part of the basic process these problems may go unnoticed and often only become clear if the point cloud is examined.

(4) Surfacing (Error-4). As discussed in the previous section surface meshes can be applied to a point cloud to improve its visualisation. The mathematics of different surfacing algorithms varies and therefore their ability to preserve 3D features could in theory vary.

If a model is scaled accurately then in theory a linear dimension between two points on the original surface should be identical in value to the dimension between the same two points on the 3D model. Equally take a network of points and the distances between should be the same if the points are placed correctly in 3D space when comparing the original to model. Both Error-1 and -2 are in play. A pragmatic solution to check for scaling accuracy is to put an object with known 3D dimensions onto a surface prior to model building, or alternatively use that object to create an impression on the surface slightly away from the evidential marks. Lego bricks have universal dimensions, do not expand or contract, and are ideal for this purpose. In particular Lego Duplo™ Blocks have the added advantage of being larger (Fig. 3).

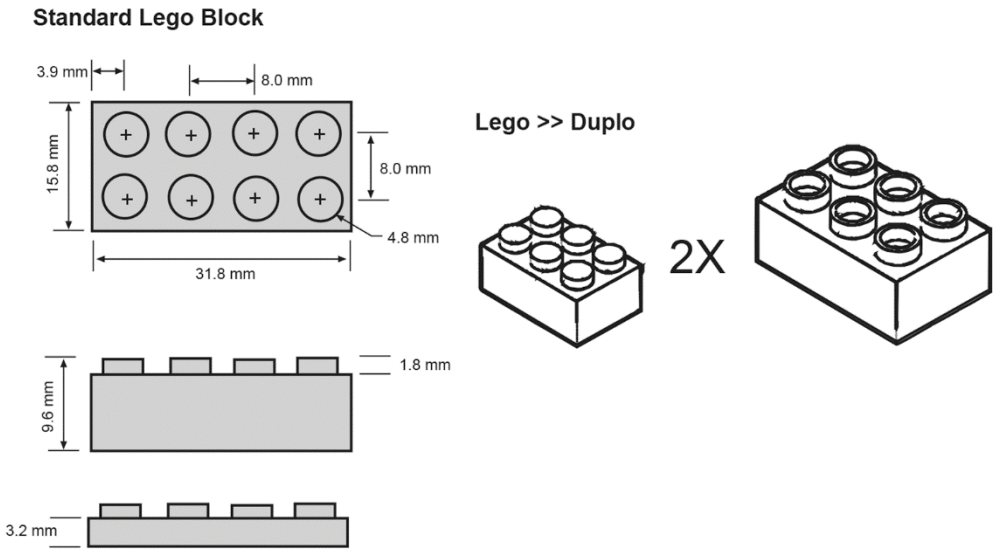

Figure 3: Standard dimensions of Lego blocks which due to their abundance and modular nature are ideal for checking model accuracy.

A simple and quick calibration test for the photogrammetry process in conjunction with DigTrace can be undertaken using a Lego or Duplo brick. If a brick is pressed into a medium such as mud, or wet sand, then it will create a perfectly square outline. The authors would recommend doing this regularly not necessarily at a scene but in similar environments to those commonly faced to establish the accuracy for *their* individual setup. Variation in accuracy is likely to be small as shown by a simple experiment. Lego blocks were pressed into a sheet of Bubber™, a non-drying modelling compound similar to playdough previously identified for its potential for taking test impressions [26]. Models were made of these impressions using six different cameras using the standard DigTrace protocol [3]. Digital measurements were taken from the 3D point cloud for each scenario and compared with the physical measurements of the Duplo brick (Table 2). Maximum errors range from 0.16 to 1.245 mm, with a mean maximum error of 0.496 ± 0.073 mm across all the cameras. Given that the size between shoe sizes is 8.46 mm (one barleycorn) this equates to a potential worse case error of ±14.7%. This errors is not just that associated with different cameras, although it does indicate that the method is not particularly sensitive to the camera used, but also includes the algorithm (Open MVG in this case) and errors associated with the operator at all stages. The point here is that every individual practitioner, and equipment setup, should calculate these errors for their particular operational practice.

Camera	Sensor Width (mm)	Measurement-1 (31.8 mm)	Measurement-2 (44 mm)	Measurement-3 (25 mm)
iPhone XS Max	5.8	31.1 [± 0.1]	43.91 [± 0.07]	25.2 [± 0.12]
Sony A7	23.5	30.89 [± 0.02]	43.6 [± 0.06]	24.43 [± 0.1]
Sony A6000	35.7	31.02 [± 0.15]	44.08 [± 0.16]	25.67 [± 0.12]
Cannon EOS 5D	35.8	31.64 [± 0.19]	43.34 [± 0.59]	25.26 [± 0.09]
Cannon EOS 1200D	22.3	31.4 [± 0.14]	44.5 [± 0.086]	25.2 [± 0.07]
Nikon D200	23.6	31.7 [± 0.18]	44.12 [± 0.058]	25.14 [± 0.068]

Table 2: Average measurements from multiple cameras of a Duplo block impression made in the modelling compound Bubber (N = 5). Each 3D model was composed of 25 photographs, scaled and autorotated so it was perpendicular to the orthogonal plane. Mesurement-1 corresponds to the length of a four-stud block; Measurement-2 to the diagonal of a four-stud block; and Measurement-3 corresponds to the inside dimension between two re-entrants on the underside of a four-stud block.

Absolute accuracy is important but so is the reproducibility of results. The statistics of sampling suggests that error rates should fall and precision increase as the sample size increases to the limits of any given operator, equipment, or measurement protocol (Fig. 4). A user would rarely have the time to make multiple 3D models of the same target and as a consequence these errors are not easily measured. However, this approach can be used to calculate a measure of precision for a given protocol and footwear evidence type which would be applicable to all similar circumstances. A precision rate of this type should in theory only vary with preservation environment assuming that camera, software, protocol, and operator remain unchanged.

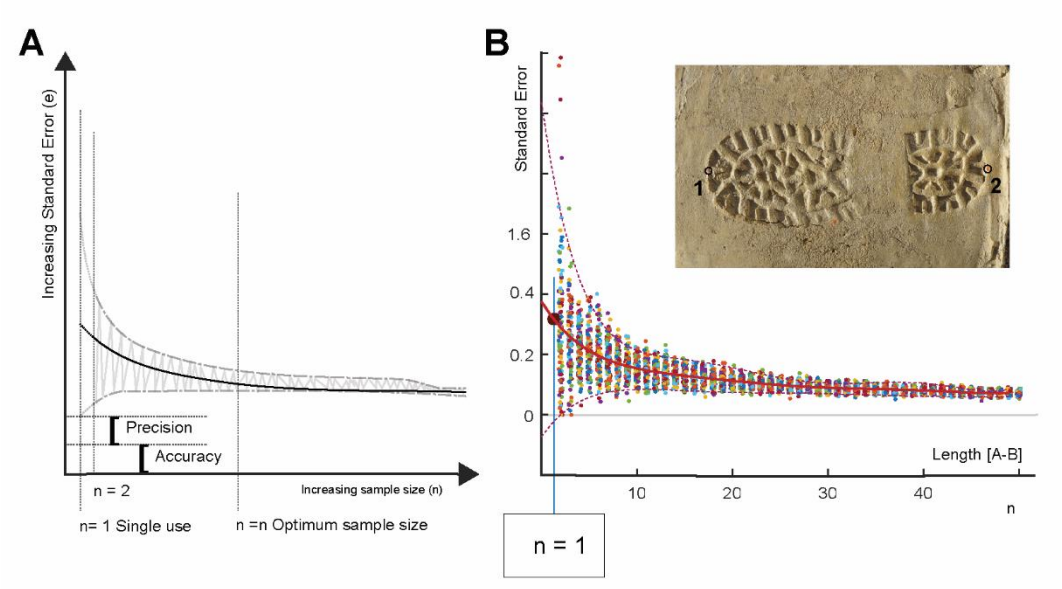

*Figure 4: Estimating precision for one-time recovery using SfM. A. Conceptual model showing how error rates should decrease as sample size increases. B. Application to a shod concrete track, illustrated, for SfM models made via photogrammetry and DigTrace (*www.digtrace.co.uk*).*

A precision value can be calculated by replicating the complete photogrammetry process: capture, 3D model building, scaling and measurement between known points at least 20 times or more (Fig. 4). This should be done for each environment in which models are typically captured by the practitioner in question. To measure precision networks of landmarks are pre-placed on the tracks before recovery. The target is then photographed to create the first 3D model according the protocol being used. The operator then stands up, walks away and resets, before coming back to the target and repeating the recovery steps. This is repeated at least 20 (N) times, preferably 50, to build up the data needed to generate an error model. Each set of photographs is used in isolation to generate a 3D model, which is scaled, and digital linear measurements taken between the known points on the 3D model. You end up with N models and N measurements. Using these measurements, you can calculate the errors using the following analytical procedure. https://github.com/bosmart/sfm-paper

(1) Generate N = 100 bootstrap samples (with replacement) for each value of k in the range between 2 and 50.
(2) Calculate the Standard Error (SE) for each bootstrap sample and each value of k (scatter plot in Fig. 4B).
(3) Derive the mean and standard deviation from SE values for each value of k.
(4) Fit polynomial curves to the means and 95% confidence interval (CI) boundaries of the normal distributions calculated in Step 3 above (the CI values were clipped at 0 prior to curve fitting, see the solid and dashed lines in Fig. 4B).
(5) Estimate the SE and its CI's for K=1 by extrapolating the curves obtained in step 4 above (see the blue vertical line in Fig. 4B).

Table 3 compares a range of precision estimates for length and width measurements taken from footwear impression made in different environments with 3D models generated in DigTrace. A singular use of an optical laser scanner (Next Engine) has been included alongside the values produced via SfM photogrammetry to illustrate comparative values. These errors include all aspects in the recovery from operator, equipment, and protocol. The mean error across all environments for length is 1.615 ±0.729 mm with a maximum error of 6.445 mm and a minimum of 0.322 mm. Width gives better results (0.681 ±0.284 mm) as does the distance between key point inside the footwear impression (0.358 ±0.048 mm; Table 3). A single model with all other recovery variables held constant will give precision on most measurements of the order of 0.35 ±0.048 mm. The reason for the higher values in terms of length largely comes from the nature of the tracks used. Modern sports shoes tend to curve front and back which can make defining the start and end of a track difficult. If there are undercut edges, there may also be missing points in the SfM model in these areas. Measurements on the point cloud are always between individual points (i.e. not interpolated between points). The width values show less variation since these are typically easier to define and less disturbed. There is also variability between environments, note the low precision values for the gypsum sand, and for Mud-1 (Table 3). The gypsum sand is extremely white

and highly reflective as such the pixel uniformity in the images is challenging for the pixel matching algorithms OpenMVG used here. Equally Mud-1 was an extremely damp print with a complex toe area overhung by vegetation. Reflection from damp surface causes placement errors during the SfM computation and the complex overhung toe area is imaged slightly differently each time depending on the specific orientation of the photographs taken. If a photograph is taken slightly lower or with better line of sight into an overhung area in one set of model-building images compared to the next, then subtle differences in the model build will result. The lower levels of precision for the snow models reflects the challenge that this environment can pose for SfM due to the uniformity of image pixels and the potential for reflection/refraction. The more texture the snow has, coupled with consistent low-elevation illumination the better the results will normally be. In general, these precision measurements compare favourable to those obtained by the used optical laser scanner (Table 3). As with absolute accuracy precision estimates can easily be made using the above process by a practitioner and established for their particular equipment, protocol, and the typical environments from which they recover 3D footwear impressions.

	Surface Environment	Average Length Error (mm)	95% Maximum Length Error (mm)	Average Width Error (mm)	95% Maximum Width Error (mm)	Average KP Error (mm)	95% Maximum KP Error (mm)
Next Engine 3D scan	Modelling clay	0.78	2.13	0.42	1.16	0.35	0.89
DigTrace	Builder sand	0.46	1.20	0.26	0.68	0.35	0.93
	Gypsum sand	2.28	6.01	2.60	6.65	0.58	1.70
	Mud 1	6.44	17.92	0.40	1.10	0.29	0.75
	Mud 2	0.50	1.31	0.23	0.63		
	Mud 3	0.40	1.05	0.32	0.82	0.24	0.64
	Snow 1	1.38	3.69	0.79	3.20	0.37	0.95
	Snow 2	1.14	2.91	0.67	1.77		
	Concrete	0.32	0.82	0.17	0.45	0.32	0.82

Table 3: Error rates for length, width, and distance between known points for a single operator across a range of surface environments. Note the results of a next Engine are provided for comparison.

The third type of error recognised above (Error-3) is the absence of points in the cloud. These are only visible in the cloud itself and are often obscured by surfacing/meshing algorithms which can fill small holes or gaps (Fig. 2B). Such meshes are basically a mathematical representation of the surface of the cloud of points. If there is no data, then there is a potential for error in the model. We have already discussed above the potential causes of holes such as surface uniformity and reflectivity. Figure 5 shows the results of two 3D models made of the same clay footwear impression. In one case the photographs were taken in poor light conditions and in the second the model was taken in better light. By counting the number of pixels in a unit area of the cloud (0.5 mm grid) we can identify those areas with redundancy in terms of points and those where there are few points. This type of Quality Assurance check is

not routine within SfM software but can computed using python code written by one of the authors available at https://github.com/bosmart/sfm-paper. A '.csv' file is used as input with three data columns corresponding to the x, y and z coordinates of the points, most 3D software will export the point cloud in this way. The model created in the better light conditions (Fig.5B) has a better coverage of points and the histogram of points per unit area is positively skewed. We can also see that the variation in z-values (elevation) is slightly less in the better lite model. If the area of maximum interest in a model has a consistent and high point density, then it is likely to follow the surface with a high degree of fidelity. If, however it does not then inference about track topology in blank areas may be more suspect. Ideally one wants a count per unit area that shows a positive or peaked kurtosis (leptokurtic) and with a negative skew; that is a histogram that has a high number of cells with a maximum point count and few with a low point count (Fig. 5B). It is possible to compare different models in this way using the histograms as a first order guide provided the count is normalised by model area. It is important to note however that simply having a large point count is not necessarily always a good thing. An undercut surface displayed in this way would give a high point count because you would count both the upper surface and the points in the undercut below. Equally a noisy model with lots of spurious surface points would give a high point cloud density but could give a poor model when surfaced. We can check for this by looking at the variance in z-values by unit area (Fig. 5). High variance should occur in those areas with maximum roughness and ideally one is looking for both a leptokurtic distribution and a positive skew or tail when looking at the histogram.

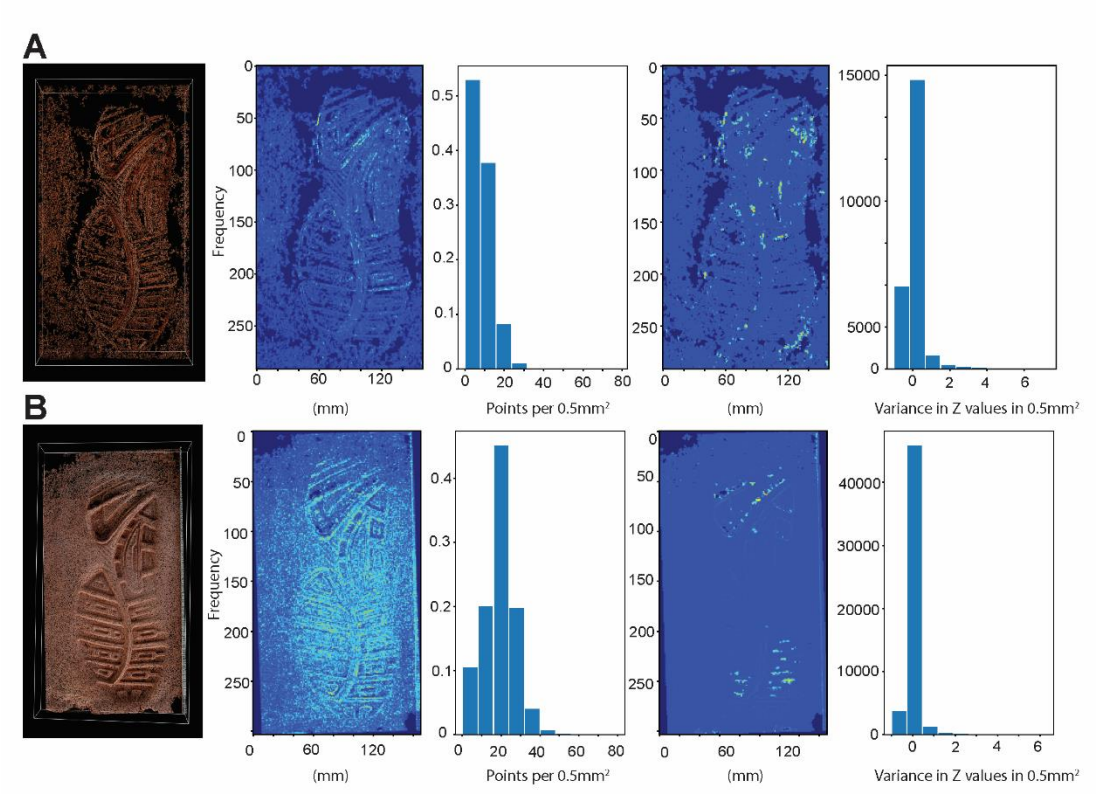

Figure 5: Comparison of the same subject via two different models of varying quality (captured under different light conditions). ***A.*** *Outputs from model captured in low light.* ***B.*** *Outputs from*

model captured in brighter even light. The first two columns show the point cloud distribution, the middle column shows the point count per 0.5mm2 while the right two columns refer to the Z values and show the distribution followed by the variation in z values within 0.5mm2.

The final type of potential error identified above is associated with the mathematical surfacing algorithm used (Error-4). To explore the significance of this potential error a comparison of two common surfacing techniques (2.5D Delaunay Triangulation and Poisson Surface Reconstruction) was undertaken (Fig. 2). A mesh to mesh comparison undertaken in Cloud Compare gives a mean difference between two point on the mesh of only ± 0.007 mm and a standard deviation of 0.097 mm. So, while this error is included for completeness its contribution is small.

3 Application

The aim here is to simply demonstrate what can be achieved for a range of depositional environments and simple scenarios. In built-up areas 3D footwear impressions are commonly found in sand or mud along roadside verges, gutters, access paths/tracks, or in flower beds. These types of trace, if identified for recovery, are usually captured via 2D vertical photography, and rarely cast due to the time and effort, and therefore expense involved, at least in the UK. The advantage of using SfM as a complimentary recovery technique is that it takes literally just over a minute to collect the additional photographs at a scene and in contrast to scanning no specialist equipment is needed. Even if the model subsequently fails to build, which is rare, or has several data-poor patches, you have lost nothing except a small amount of time, but you have potentially gained a significant additional data source. Perhaps most importantly the trace can be revisited effectively in situ multiple times as an investigation develops. You can view this trace from different angles and also use different depth-colour renders to pick out detail and unlike a 2D photograph you can also measure depth directly (Fig. 6).

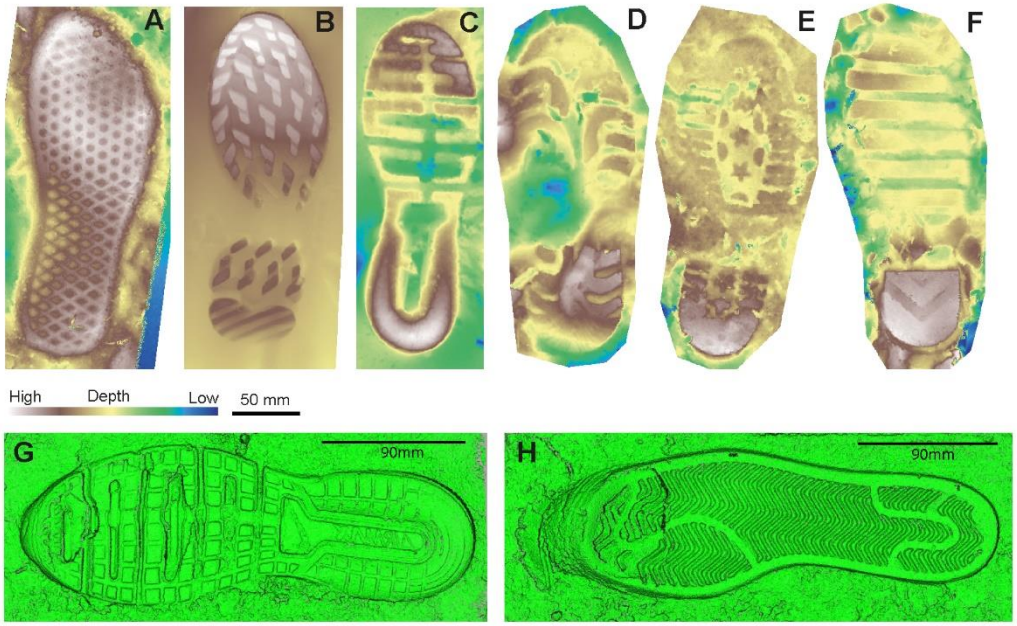

Figure 6: A selection of footwear impressions left in natural settings. The 3D SfM models are depth-colour rendered and viewed vertically from above. Three footwear impression were made in sand (A, Size 6 Vans Female. B, Size 6 Adidas Female. C, Size 6 Nike Female) and three in natural soil (D, unknown. E, unknown. F, Generic wellington boot, size unknown). The models were created in DigTrace, scaled, cropped and auto-rotated such that the surface is orthogonal to the viewing plane. The depth colour render used here is 'terrain'. G, example of a sand impression. Size 6 Nike Air, using a one colour render in CloudCompare. H, example of a sand impression, size 6 Adidas, using a one colour render in CloudCompare.

Models such as those in Figure 6 can be used to take digital measurements as illustrated by the following example. Simple impressions in a flower bed where made with two identical shoes except for their size, Shoe A (Female, UK Size 6), and Shoe B (Male UK Size 11). Photographs were collected for an SfM model using an iPhone XS Max and a Sony A7 mirrorless camera. The models created were scaled and auto-rotated within DigTrace and then measured using a digital measuring tool (Table 4). The shoes, impression and consequent three-dimensional models were all measured for comparison. The results indicate a high level of accuracy when using different cameras and highlight that models can be differentiated from one another based on measurements if multiple impressions are found that appear to be the same pattern but are in fact different size shoes and therefore the impressions made from different sources. The disparity between models A and B shows a difference of 41 mm (length) correlating with the 45 mm disparity between the physical shoe size lengths.

	Model photographed by Sony A7 - Length	Model photographed by Sony A7 - Width	Model photographed by Iphone XS Max - Length	Model photographed by Iphone XS Max - Width	Physical Impression Length	Physical Impression Width
Shoe A impression	286.99mm	78.14mm	286.13mm	78.21mm	290mm	75mm
Shoe B impression	326.42mm	81.39mm	329.26mm	83.45mm	330mm	80mm

Table 4: Comparison of two shoe impressions using digital measurements taken from different SfM models of these impressions.

Traces can also be compared to other traces left at a crime scene and compared directly to a SfM model of a test impression made with a suspect's shoe in a modelling medium such a Bubber™ [26], or directly to an SfM model of the outsole of a suspect's shoe. Within DigTrace this is achieved using a comparison function which allows the user to match pairs of points between two models [3]. Typically, these points are the outer-dimensions of an impression. The software then computes a transformation of one track to the other by minimising the mean squared deviation between the landmark coordinates in the x-y plane [3,27]. Transformation can either be rigid or affine, the former preserving aspects of size and is therefore most appropriate in forensic work, while the latter focuses on shape alone. Once two or more traces are co-registered the software then samples the stack of superimposed tracks to compute a frequency distribution of values for each point over the surface. These values be used to calculate a mean 3D track for a group of similar tracks on trackway or used to compare the statistical difference between two tracks [3]. Take the tracks in Figure 7 made in sand by identical boots with different levels of wear. By superimposing the tracks, we can focus attention not just on areas of difference but also on the degree of statistical difference. Figure 7C is the standard deviation of points when the two tracks are compared, we can set a threshold across this to pick out those which are statistically significant at 95%. In this case the wear differences around the heel are statistically different.

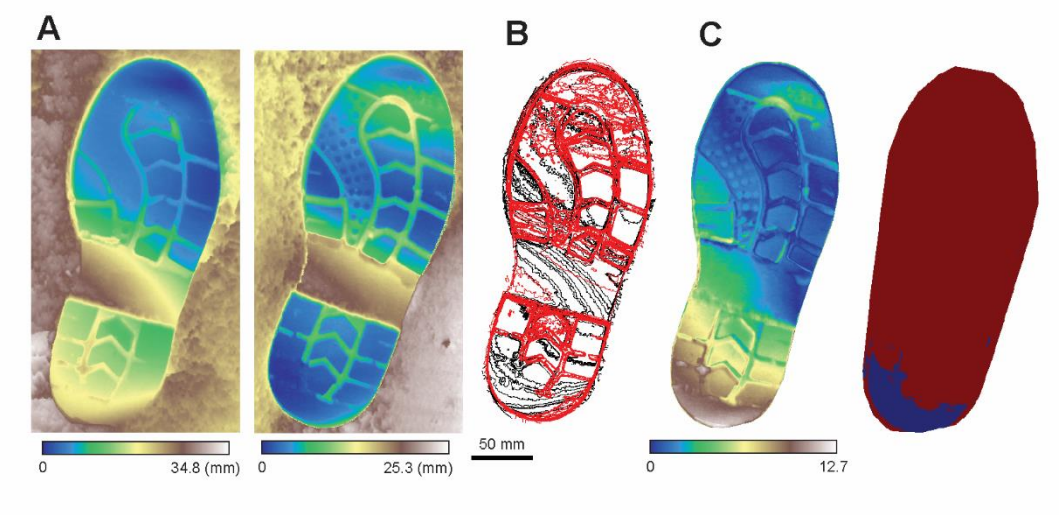

Figure 7: Statistical comparison of two shoes with different levels of wear. ***A.*** *Shoe prints made in sand, captured in 3D and depth-colour rendered.* ***B.*** *Contour lines (1 mm) showing the difference between the two tracks when co-registered.* ***C.*** *The standard deviation between the two co-registered shoe prints and a version with a 2 standard deviation threshold applied showing areas (blue) that show a statistical variance greater at 95% [3].*

An SfM approach works across a range of substrates from traditional sand, mud, and soil, while also having potential for substrates that are often regarded as difficult to cast such as loose sand or snow [28,29,30,31,32]. Figure 8 illustrates this in the context of loose, sandy gravel found on a path on a local nature reserve. The vertical photograph while picking up some of the class characteristics of the impression does not give as much detail as the depth-colour rendered or surfaced versions and both give superior results to a dental stone cast. SfM also offers a solution for 3D recovery of traces in snow, although due to surface reflection and potential pixel uniformity in snow there is a risk of models not building. Figure 8 shows SfM models of sufficient quality to capture class characteristics and in some cases randomly acquired characteristics (RAC; Fig. 9). The key is to avoid sparkling reflections, while keeping some textural variation in the form of shadows within the track. As the snow ages, especially in a country such as the UK, the textural diversity increases and so does the quality of the 3D models. Flat uniform light is often a problem.

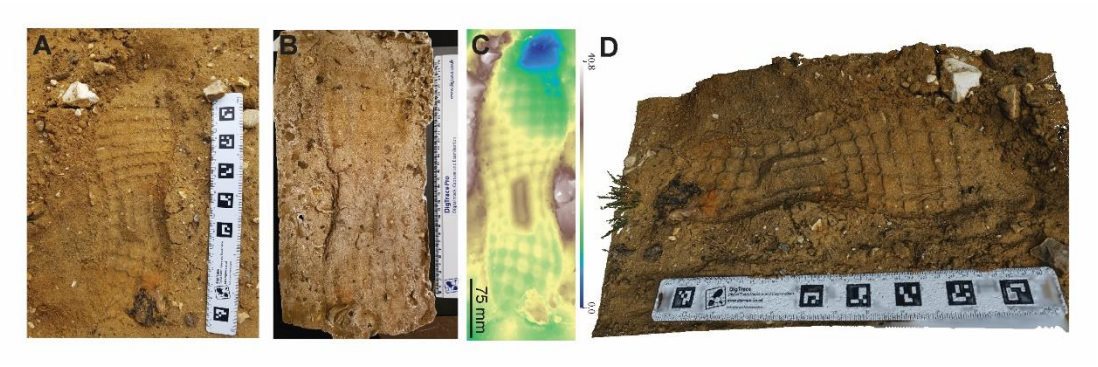

Figure 8: A footwear impression made in a loose, sandy gravel substrate. ***A.*** *Original impression viewed from above.* ***B.*** *Dental stone cast of the impression.* ***C.*** *Depth-colour rendered SfM model of the impression.* ***D.*** *Surfaced SfM model of the impression that can be rotated and viewed from different angles or positions.*

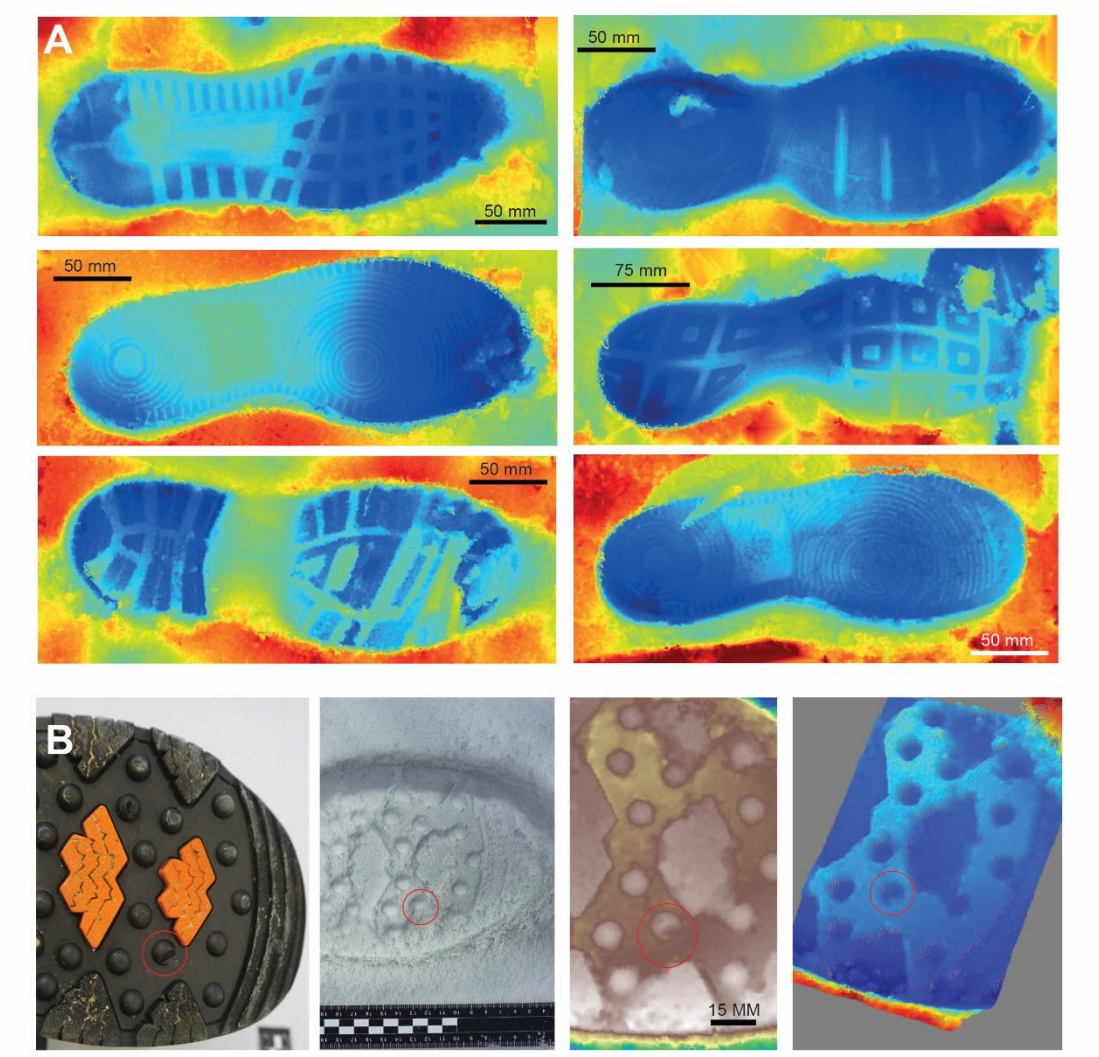

Figure 9: SfM models of footwear impression in snow. A. Series of impressions with different shoes taken in snow. In the depth colour render warm colours correspond to high areas and cool colours to low areas. B. Shoe with RAC circled in red, alongside a photograph of the snow track and then two SfM colour-rendered models. The first model has a depth scale of green/brown colours corresponding to high areas and grey colours corresponding to low areas. The final model is orientated at an oblique angle to highlight the subtle feature of interest, depth scale as in 9A.

4 Discussion: the way forward

In the previous section we have illustrated how an SfM approach can be used to recover a range of 3D footwear traces across different track preserving environments. These techniques are routinely used in the analysis and preservation of fossilised vertebrate traces (ichnology), including human tracks, and digital methods are now considered to be the scientific standard for recovery and preservation of such evidence [e.g., 33,34]. The vertebrate ichnological

community has become to agree basic standards of data reporting, presentation, and archiving [35]. This, coupled with increased awareness, has led to a rapid growth in the number of footprint discoveries around the world in last five years. The same methodological revolution could follow in forensic practice given more widespread experimentation and adoption of SfM as a complimentary method to those already used in forensic practice for the recovery of footwear evidence.

To aid this we have reviewed the workflows and discussed potential sources of error. In particular we have drawn attention to how CSI practitioner can determine both the accuracy and precision of a SfM solution using their own combination of equipment, software, and collection protocol. There is a risk that models, built once the scene is left, do not build correctly due to problems of surface textural uniformity or reflection from wet surfaces. This is no different however than the risk that cast either damages or fails to preserve the available detail since the process of casting is usually a one-time destructive process. In both cases, SfM and casting recovery, experiential learning is important and ultimately the key to success. A successful SfM model has significant advantages over more traditional casts, since casts are bulky making them difficult to store, analyse digitally, and share quickly. Perhaps the key advantage, however, of SfM models is the ability to colour-render with depth to bring out different features and to provide a means of statistical testing the differences between two traces. SfM based recovery also works in environments that are traditionally difficult to cast such as in snow, and loose, dry sandy substrates [36].

A high quality forensic-grade 2D photograph will often be sufficient for most investigative needs and give as much detail as a SfM model in the x-y plane. While photographs can give accurate measurements in the x-y plane depth comparisons and measurements are much harder. Moreover the CSI practitioner determines the angles and viewpoints at the point of capture in the case of a 2D photograph, but a 3D SfM model can be revisited many times and viewed from different angles with different depth-colour renders and with different illumination angles and brightness. The key is not to consider SfM as an alternative but as an additional and complimentary recovery method which at least at the scene involves little additional effort. Table 5 summaries the relative merits of existing recovery techniques for 3D footwear impressions and compares them to those of an SfM based approach.

Tuttle [37,38] made a number of clear and valid recommendations with respect to the introduction of new forensic methods with specific reference to the interpretation of barefoot prints at crime scenes, namely: (1) that any data and methods by self-proclaimed footprint experts need to be rigorously peer reviewed outside the court room before they enter it; (2) that the credentials of foot experts need to be certified and verified in some way as well as being limited to their area of expertise; and (3) all new forensic tools need to be subject to rigorous scientific testing before they are applied in criminal cases. These principles are not that different from the guidelines issued by the US Supreme Court in light of the Daubert v. Merrill Dow Pharmaceuticals, Inc. (1993) that new techniques and expert opinions need to:

(1) have established methods; (2) have a known or potential error rate; (3) have widespread acceptance by the relevant scientific community; (4) have been subject to peer review; and (5) be testable and have been tested through scientific method. We can apply these tests to the use of SfM photogrammetry in the recovery of footwear evidence. This paper sets out the basic workflows associated with the use of SfM photogrammetry in forensic practice building on the work of others [e.g., 3,39,40,41]. The method has levels of accuracy and precision that can be determined for a specific camera, collection protocol, camera, practitioner, substrate, and software as set out in this paper. The use of objects of known size, coupled with estimating the maximum and minimum error rates as set out in Figure 4 and reported for the author's setup in Table 3, shows the way. Larsen and Bennett [18] also reviewed the errors associated with SfM recovery of footwear impressions.

In terms of widespread acceptance within the forensic community this is currently lacking. However in the study of vertebrate ichnology, including human tracks, SfM recovery is now considered to be standard and is routinely used by almost all practitioners [e.g., 33,42-49]. In fact, a paper on a set of fossilised tracks would not be accepted for publication without some form of 3D analysis whether by optical laser scanning or SfM photogrammetry, it is the accepted norm [35]. Practitioners have already come together to define best practice in terms of the collection and presentation of 3D data [35]. The forensic community is behind the curve on this. SfM methods and associated analytical/statistical techniques using digital tracks created in this way have been subject to extensive peer review as the sheer number of publications testifies, six fossilised human track papers in the first nine months of 2020 alone. Cross-disciplinary transference of methodological practice is slow in all fields, but it is perhaps timely for the forensic footwear community to acquaint themselves with this work and learn from it [3].

It is the final Daubert test that we would argue needs significant further work, that the methods should be tested through application of the scientific method. This is certainly true in the context of fossil traces but is perhaps lacking in forensic practice. This may reflect a decreasing emphasis placed on footwear evidence by some forensic organisations and police forces, something which is true in the UK at least, despite the ubiquity of such evidence, but is also a function of the inherent inertia of changing established methods and approaches. We would suggest that there is a need for operational-based comparative testing of SfM based recovery so that it can be compared to other methods so that the advantages, pitfalls and comparative errors can be established leading to an operational analysis of the cost benefit of embracing an SfM based approach can be established. Papers like this one play a role in illustrating the potential of new techniques, but true operational trials require the practice-based community to participate. We call upon the forensic footwear community to embrace this need.

Method	Cost	Training	Speed	Output	x, y data	x, y, z data	Invasive?	Risk?	Storage/Sharing
SfM	Scene: low, existing CSI cameras used. Lab: medium, investment in IT and software.	Scene: medium training for CSI, mainly awareness Lab: high, training of specialist officers to gain full analytical potential.	Scene: fast, *circa*. 70 seconds per target. Lab: slow, *circa*. an hour to build and analyse a model.	Digital 3D model, can be 3D printed if needed.	Yes (D)	Yes (D)	Non-invasive	Medium	Digital models easily stored and shared by file transfer systems.
Casting	Scene: low, consumables only. Lab: low consumables only.	Scene: low, mainly experiential. Lab: medium, mainly experiential.	Scene: slow, up to 45 minutes per target depending on prevailing conditions Lab: slow, adhering trace evidence needs to be considered first, cast then needs to be dried and cleaned.	Artefact	Yes (A)	Yes (A)	Invasive	Medium	Storage of bulky artefact, difficult to share quickly.
Photography	Scene: low, existing CSI cameras used. Lab: medium, investment in IT and software.	Scene: medium, good quality photographs require training. Lab: medium, training of specialist officers to gain full analytical potential.	Scene: medium, depends on the target and conditions. Lab: medium, time to scale, prepare and analyse individual photographs	Digital image	Yes (D)	No	Non-invasive	Low	Digital images are easily stored and shared by file transfer systems.
Laser Scanning	Scene: High, specialist equipment. Lab: medium, investment in IT and software.	Scene: high, training needed for SCI. Lab: high, training of specialist officers to gain full analytical potential.	Scene: Impressions can be captured in under a minute with some scanners, with preparation taking more time. Not typically totalling more than five minutes. Timings vary with type/make/model of scanner used. Lab: Dependant on scanner, a 3D mesh can be directly available for use in analysis	Digital 3D model, can be 3D printed if needed.	Yes (D)	Yes (D)	Non-invasive	Low	Digital models easily stored and shared by file transfer systems.

Table 5: Summary of the relative merits to different 3D recovery techniques. Note that risk is this context is the risk on non-recovery of evidence, (D) is digital measurements and (A) is analogue measurement

5 Conclusion

We suggest that the use of SfM Photogrammetry for forensic practice in the recovery of 3D footwear traces forms a useful and complimentary method to existing methods especially to 2D photographic capture. What is now needed is community based operational trials and tests to build confidence in the approach and we call upon the forensic footwear community to embrace this idea.

Automated pattern matching to supplement, or even replace the footwear expert, has been a goal for some years with varying degrees of success [3]. Developments in machine learning make these goal more achievable, and rapid matching algorithms are already available. For example, Henderson et al. [5] have shown how digital custody capture linked to rapid searches of recently recovered traces has significant potential for intelligence led policing. In particular it allows a suspect's footwear to be rapidly linked, at least by their class characteristics, to local traces in a timely fashion allowing officers to broaden the scope of an investigation while interviewing that suspect. The input is currently limited to black and white 2D traces, but 3D models colour rendered appropriately can be integrated quickly into these systems, perhaps more quickly than 2D photographs with their complex tonal variability. In summary we would argue, especially in light of the transformation which has occurred in the study of fossilised traces using SfM, that the future promise of footwear recovery via SfM is bright.

References

[1] NPIA (National Policing Improvement Agency), Footwear Marks Recovery Manual, 2007. http://library.college.police.uk/docs/appref/NPIA-(2007)-Footwear-Marks-Recovery-Manual.pdf.

[2] W.J. Bodziak, Forensic Footwear Evidence, CRC Press, Boca Raton FL, 2017. https://doi.org/10.1201/b19479.

[3] M.R. Bennett, M. Budka, Digital technology for forensic footwear analysis and vertebrate ichnology, Springer International Publishing, 2018. https://doi.org/10.1007/978-3-319-93689-5.

[4] U. Buck, K. Bußе, L. Campana, C. Schyma, Validation and evaluation of measuring methods for the 3D documentation of external injuries in the field of forensic medicine, Int J Legal Med. 132 (2017) 551-561. https://doi.org/10.1007/s00414-017-1756-6.

[5] J. Henderson, R. Armitage, If the Shoe Fits: Proposing a Randomised Control Trial on the effect of a digitised in-custody footwear technology compared to a paper-based footwear method., Crime, Secur. Soc. 1 (2018). https://doi.org/10.5920/css.2018.02.

[6] U. Buck, N. Albertini, S. Naether, M.J. Thali, 3D documentation of footwear impressions and tyre tracks in snow with high resolution optical surface scanning, Forensic Sci. Int. 171 (2007) 157–164. https://doi.org/10.1016/j.forsciint.2006.11.001.

[7] M.R. Bennett, D. Huddart, S. Gonzalez, Preservation and analysis of three-dimensional footwear evidence in soils: The application of optical laser scanning, in: Crim. Environ. Soil Forensics, Springer Netherlands, 2009: pp. 445–461. https://doi.org/10.1007/978-1-4020-9204-6_28.

[8] S. Ullman, The interpretation of structure from motion, Proc. R. Soc. London. Ser. B. Biol. Sci. 203 (1979) 405–426. https://doi.org/10.1098/rspb.1979.0006.

[9] R. Hartley, A. Zisserman, Multiple View Geometry in Computer Vision, Cambridge University Press, 2004. https://doi.org/10.1017/cbo9780511811685.

[10] M.J. Westoby, J. Brasington, N.F. Glasser, M.J. Hambrey, J.M. Reynolds, “Structure-from-Motion” photogrammetry: A low-cost, effective tool for geoscience applications, Geomorphology. 179 (2012) 300–314. https://doi.org/10.1016/j.geomorph.2012.08.021.

[11] M.A. Fonstad, J.T. Dietrich, B.C. Courville, J.L. Jensen, P.E. Carbonneau, Topographic structure from motion: A new development in photogrammetric measurement, Earth Surf. Process. Landforms. 38 (2013) 421–430. https://doi.org/10.1002/esp.3366.

[12] M.W. Smith, J.L. Carrivick, D.J. Quincey, Structure from motion photogrammetry in physical geography, Prog. Phys. Geogr. Earth Environ. 40 (2016) 247–275. https://doi.org/10.1177/0309133315615805.

[13] M. Pollefeys, R. Koch, M. Vergauwen, L. Van Gool, Automated reconstruction of 3D scenes from sequences of images, ISPRS J. Photogramm. Remote Sens. 55 (2000) 251–267. https://doi.org/10.1016/S0924-2716(00)00023-X.

[14] F.A. Andalo, F. Calakli, G. Taubin, S. Goldenstein, Accurate 3D footwear impression recovery from photographs, in: Institution of Engineering and Technology (IET), 2012: pp. P24–P24. https://doi.org/10.1049/ic.2011.0121.

[15] R.E. Gamage, A. Joshi, J.Y. Zheng, M. Tuceryan, A high resolution 3D tire and footprint impression acquisition for forensics applications, in: Proc. IEEE Work. Appl. Comput. Vis., 2013: pp. 317–322. https://doi.org/10.1109/WACV.2013.6475035.

[16] C. Villa, C. Jacobsen, The application of photogrammetry for forensic 3D recording of crime scenes, evidence and people, in: Essentials Autops. Pract. Rev. Updat. Adv., Springer International Publishing, 2020: pp. 1–18. https://doi.org/10.1007/978-3-030-24330-2_1.

[17] T.J.U. Thompson, P. Norris, A new method for the recovery and evidential comparison of footwear impressions using 3D structured light scanning, Sci. Justice. 58 (2018) 237–243. https://doi.org/10.1016/j.scijus.2018.02.001.

[18] H.J. Larsen, M.R. Bennett, Empirical Evaluation of the Reliability of Photogrammetry Software in the Recovery of Three-Dimensional Footwear Impressions, J. Forensic Sci. 65 (2020) 1722–1729. https://doi.org/10.1111/1556-4029.14455.

[19] P. Moulon, P. Monasse, R. Perrot, R. Marlet, OpenMVG: Open multiple view geometry, in: Lect. Notes Comput. Sci. (Including Subser. Lect. Notes Artif. Intell. Lect. Notes Bioinformatics), Springer Verlag, 2017: pp. 60–74. https://doi.org/10.1007/978-3-319-56414-2_5.

[20] Ultimate List of Free Photogrammetry Software | 3D Knowledge, (n.d.). https://3dknowledge.com/free-photogrammetry-software/ (accessed November 16, 2020).

[21] 2020 Best Photogrammetry Software (Some are Free) | All3DP, (n.d.). https://all3dp.com/1/best-photogrammetry-software/ (accessed November 16, 2020).

[22] M. Kazhdan, H. Hoppe, Screened poisson surface reconstruction, ACM Trans. Graph. 32 (2013) 1–13. https://doi.org/10.1145/2487228.2487237.

[23] B. Delaunay, Sur la sphere vide, Bull. l'Académie Des Sci. l'URSS. 6 (1934) 793–800.

[24] D.T. Lee, B.J. Schachter, Two algorithms for constructing a Delaunay triangulation, Int. J. Comput. Inf. Sci. 9 (1980) 219–242. https://doi.org/10.1007/BF00977785.

[25] F. Remondino, R. Fabio, International Archives of the Photogrammetry, Remote Sens. Spat. Inf. Sci. XXXIV-5/W10 (2003). https://doi.org/10.3929/ethz-a-004655782.

[26] J. LeMay, Making three-dimensional footwear test impressions with "bubber," J. Forensic Identif. 60 (2010) 439-448.

[27] M.R. Bennett, S.C. Reynolds, S.A. Morse, M. Budka, Laetoli's lost tracks: 3D generated mean shape and missing footprints, Sci. Rep. 6 (2016) 1–8. https://doi.org/10.1038/srep21916.

[28] T.W. Adair, R.L. Shaw, The dry-casting method: A reintroduction to a simple method for casting snow impressions, J. Forensic Identif. 57 (2007) 823-831.

[29] T. Adair, Capturing Snow Impressions, Law Order. 57 (2009) 14-16.

[30] L. Hammer, J. Wolfe, Shoe and Tire Impressions in Snow: Photography and Casting, 2003.

[31] N. Petraco, H. Sherman, A. Dumitra, M. Roberts, Casting of 3-dimensional footwear prints in snow with foam blocks, Forensic Sci. Int. 263 (2016) 147–151. https://doi.org/10.1016/j.forsciint.2016.03.033.

[32] J.R. Wolfe, Sulfur cement: A new material for casting snow impression evidence, J. Forensic Identif. 58 (2008) 485-498.

[33] M.R. Bennett, D. Bustos, D. Odess, T.M. Urban, J.N. Lallensack, M. Budka, V.L. Santucci, P. Martinez, A.L.A. Wiseman, S.C. Reynolds, Walking in mud: Remarkable Pleistocene human trackways from White Sands National Park (New Mexico), Quat. Sci. Rev. 249 (2020) 106610. https://doi.org/10.1016/j.quascirev.2020.106610.

[34] B. Zimmer, C. Liutkus-Pierce, S.T. Marshall, K.G. Hatala, A. Metallo, V. Rossi, Using differential structure-from-motion photogrammetry to quantify erosion at the Engare Sero footprint site, Tanzania, Quat. Sci. Rev. 198 (2018) 226–241. https://doi.org/10.1016/j.quascirev.2018.07.006.

[35] P.L. Falkingham, K.T. Bates, M. Avanzini, M. Bennett, E.M. Bordy, B.H. Breithaupt, D. Castanera, P. Citton, I. Díaz-Martínez, J.O. Farlow, A.R. Fiorillo, S.M. Gatesy, P. Getty, K.G. Hatala, J.J. Hornung, J.A. Hyatt, H. Klein, J.N. Lallensack, A.J. Martin, D. Marty, N.A. Matthews, C.A. Meyer, J. Milàn, N.J. Minter, N.L. Razzolini, A. Romilio, S.W. Salisbury, L. Sciscio, I. Tanaka, A.L.A. Wiseman,

L.D. Xing, M. Belvedere, A standard protocol for documenting modern and fossil ichnological data, Palaeontology. 61 (2018) 469–480. https://doi.org/10.1111/pala.12373.

[36] T. Battiest, S.W. Clutter, D. McGill, A Comparison of Various Fixatives for Casting Footwear Impressions in Sand at Crime Scenes, J. Forensic Sci. 61 (2016) 782–786. https://doi.org/10.1111/1556-4029.13044.

[37] R.H. Tuttle, Footprints: Collection, Analysis, and Interpretation. Louise M. Robbins., Am. Anthropol. 88 (1986) 1000–1002. https://doi.org/10.1525/aa.1986.88.4.02a00590.

[38] R. Tuttle, Footprint clues in hominid evolution and forensics: Lessons and limitations, in: Ichnosan Int. J. Plant Anim., Taylor & Francis Group, 2008: pp. 158–165. https://doi.org/10.1080/10420940802467892.

[39] C.D. Carlton, S. Mitchell, P. Lewis, Preliminary application of Structure from Motion and GIS to document decomposition and taphonomic processes, Forensic Sci. Int. 282 (2018) 41–45. https://doi.org/10.1016/j.forsciint.2017.10.023.

[40] G.J. Edelman, M.C. Aalders, Photogrammetry using visible, infrared, hyperspectral and thermal imaging of crime scenes, Forensic Sci. Int. 292 (2018) 181–189. https://doi.org/10.1016/j.forsciint.2018.09.025.

[41] W. Baier, C. Rando, Developing the use of Structure-from-Motion in mass grave documentation, Forensic Sci. Int. 261 (2016) 19–25. https://doi.org/10.1016/j.forsciint.2015.12.008.

[42] F. Altamura, M.R. Bennett, L. Marchetti, R.T. Melis, S.C. Reynolds, M. Mussi, Ichnological and archaeological evidence from Gombore II OAM, Melka Kunture, Ethiopia: An integrated approach to reconstruct local environments and biological presences between 1.2 and 0.85 Ma, Quat. Sci. Rev. 244 (2020) 106506. https://doi.org/10.1016/j.quascirev.2020.106506.

[43] F. Altamura, Finding Fossil Footprints in the Archival Record: Case Studies from the Archaeological Site of Melka Kunture (Upper Awash, Ethiopia), J. African Archaeol. 1 (2020) 1–10. https://doi.org/10.1163/21915784-20200011.

[44] F. Altamura, M.R. Bennett, K. D'août, S. Gaudzinski-Windheuser, R.T. Melis, S.C. Reynolds, M. Mussi, Archaeology and ichnology at Gombore II-2, Melka Kunture, Ethiopia: everyday life of a mixed-age hominin group 700,000 years ago History of Excavations, Stratigraphic Sequence and Geochronology, Sci. REPORts |. 8 (2018) 2815. https://doi.org/10.1038/s41598-018-21158-7.

[45] D. Bustos, J. Jakeway, T.M. Urban, V.T. Holliday, B. Fenerty, D.A. Raichlen, M. Budka, S.C. Reynolds, B.D. Allen, D.W. Love, V.L. Santucci, D. Odess, P. Willey, H.G. McDonald, M.R. Bennett, Footprints preserve terminal Pleistocene hunt? Human-sloth interactions in North America, Sci. Adv. 4 (2018) eaar7621. https://doi.org/10.1126/sciadv.aar7621.

[46] K.G. Hatala, W.E.H. Harcourt-Smith, A.D. Gordon, B.W. Zimmer, B.G. Richmond, B.L. Pobiner, D.J. Green, A. Metallo, V. Rossi, C.M. Liutkus-Pierce, Snapshots of human anatomy, locomotion, and behavior from Late Pleistocene footprints at Engare Sero, Tanzania, Sci. Rep. 10 (2020) 7740. https://doi.org/10.1038/s41598-020-64095-0.

[47] C.W. Helm, R.T. McCrea, H.C. Cawthra, M.G. Lockley, R.M. Cowling, C.W. Marean, G.H.H. Thesen, T.S. Pigeon, S. Hattingh, A New Pleistocene Hominin Tracksite from the Cape South Coast, South Africa, Sci. Rep. 8 (2018) 3772. https://doi.org/10.1038/s41598-018-22059-5.

[48] C.W. Helm, H.C. Cawthra, R.M. Cowling, J.C. De Vynck, M.G. Lockley, C.W. Marean, G.H.H. Thesen, J.A. Venter, Pleistocene vertebrate tracksites on the Cape south coast of South Africa and their potential palaeoecological implications, Quat. Sci. Rev. 235 (2020) 105857. https://doi.org/10.1016/j.quascirev.2019.07.039.

[49] C.W. Helm, M.G. Lockley, H.C. Cawthra, J.C. De Vynck, M.G. Dixon, C.J.Z. Helm, G.H.H. Thesen, Newly identified hominin trackways from the Cape south coast of South Africa, S. Afr. J. Sci. 116 (2020) 1–13. https://doi.org/10.17159/sajs.2020/8156.